THE JOURNAL OF BIOLOGICAL CHEMISTRY VOL. 282, NO. 24, pp. 17405–17412, June 15, 2007

Systematic Analysis of the Entire Second Extracellular Loop of the V_{1a} Vasopressin Receptor

*KEY RESIDUES, CONSERVED THROUGHOUT A G-PROTEIN-COUPLED RECEPTOR FAMILY, IDENTIFIED**

Received for publication, March 13, 2007 Published, JBC Papers in Press, April 2, 2007, DOI 10.1074/jbc.M702151200

Matthew Conner, Stuart R. Hawtin[1], John Simms[2], Denise Wootten, Zoe Lawson, Alex C. Conner[3], Rosemary A. Parslow, and Mark Wheatley[4]

From the School of Biosciences, University of Birmingham, Edgbaston, Birmingham B15 2TT, United Kingdom

The roles of extracellular residues of G-protein-coupled receptors (GPCRs) are not well defined compared with residues in transmembrane helices. Nevertheless, it has been established that extracellular domains of both peptide-GPCRs and amine-GPCRs incorporate functionally important residues. Extracellular loop 2 (ECL2) has attracted particular interest, because the x-ray structure of bovine rhodopsin revealed that ECL2 projects into the binding crevice within the transmembrane bundle. Our study provides the first comprehensive investigation into the role of the individual residues comprising the entire ECL2 domain of a small peptide-GPCR. Using the V_{1a} vasopressin receptor, systematic substitution of all of the ECL2 residues by Ala generated 30 mutant receptors that were characterized pharmacologically. The majority of these mutant receptor constructs (24 in total) had essentially wild-type ligand binding and intracellular signaling characteristics, indicating that these residues are not critical for normal receptor function. However, four aromatic residues Phe^{189}, Trp^{206}, Phe^{209}, and Tyr^{218} are important for agonist binding and receptor activation and are highly conserved throughout the neurohypophysial hormone subfamily of peptide-GPCRs. Located in the middle of ECL2, juxtaposed to the highly conserved disulfide bond, Trp^{206} and Phe^{209} project into the binding crevice. Indeed, Phe^{209} is part of the Cys-*X*-*X*-*X*-Ar (where Ar is an aromatic residue) motif, which is well conserved in both peptide-GPCRs and amine-GPCRs. In contrast, Phe^{189} and Tyr^{218}, located at the extreme ends of ECL2, may be important for determining the position of the ECL2 cap over the binding crevice. This study provides mechanistic insight into the roles of highly conserved ECL2 residues.

G-protein-coupled receptors (GPCRs)[5] exhibit a common tertiary structure comprising seven transmembrane helices (TMs) linked by extracellular loops (ECLs) and intracellular loops. The atomic detail of this generic GPCR protein fold has been reported for bovine rhodopsin (bRho). This confirmed that the chromophore 11-*cis*-retinal is covalently linked to TMVII and projects into a binding pocket formed within the TM bundle where it interacts with amino acid side chains and water molecules (1, 2). Likewise, the binding pocket for small biogenic amine neurotransmitters such as acetylcholine and norepinephrine is buried deep within the TM bundle (3). Despite this buried location of the ligand binding site, the exofacial domains of bRho are highly structured and interact with each other and with the TM helices. In particular, ECL2 of bRho forms a twisted β-hairpin structure that plunges down into the TM helical bundle to form a plug over the chromophore. There is also evidence that this ECL2 fold is not restricted to bRho and occurs in other GPCRs (4). In addition, the orientation of ECL2 in the majority of GPCRs is restrained by a conserved disulfide bond between ECL2 and the top of TMIII (1, 2).

The neurohypophysial peptide hormones vasopressin (AVP) and oxytocin (OT) are structurally related nonapeptides that generate a wide range of physiological effects, including vasopressor, antidiuretic, and uterotonic actions (5, 6). The effects of AVP/OT are mediated by a family of receptors ($V_{1a}R$, $V_{1b}R$, V_2R, and OTR), which, together with the receptors for vasotocin, mesotocin, and isotocin from lower vertebrates, constitute a sub-family of the rhodopsin/β-adrenergic receptor class of GPCRs (Family A). The $V_{1a}R$ is widely distributed and mediates nearly all of the actions of AVP with the exceptions of antidiuresis (V_2R) and ACTH secretion ($V_{1b}R$). Activation of the OTR stimulates contraction of the uterine myometrium during labor and mammary myoepithelium to elicit lactation. The $V_{1a}R$, $V_{1b}R$, and OTR couple to phospholipase C thereby generating inositol 1,4,5-trisphosphate and diacylglycerol as second messengers, whereas the V_2R stimulates adenylyl cyclase. In addition to the characteristic architecture of GPCRs, mem-

* This work was supported by grants (to M. W.) from the Wellcome Trust and the Biotechnology and Biological Sciences and Research Council. The costs of publication of this article were defrayed in part by the payment of page charges. This article must therefore be hereby marked "*advertisement*" in accordance with 18 U.S.C. Section 1734 solely to indicate this fact.

[1] Present address: Novartis Pharma AG, WSJ-386.9.59, CH-4002 Basel, Switzerland.

[2] Present address: Dept. of Pharmacology, Monash University, Wellington Road, Clayton, Victoria 3800, Australia.

[3] Present address: Institute of Life Sciences, University of Wales, Swansea SA2 8PP, United Kingdom.

[4] To whom correspondence should be addressed. Tel.: 44-121-414-3981; Fax: 44-121-414-5925; E-mail: m.wheatley@bham.ac.uk.

[5] The abbreviations used are: GPCR, G-protein-coupled receptor; AVP, [Arg^8]vasopressin; AVT, vasotocin; bRho, bovine rhodopsin; CA, cyclic peptide antagonist; D_2R, D_2 dopamine receptor; ECL, extracellular loop; InsP, inositol phosphate; $InsP_3$, inositol trisphosphate; LA, linear peptide antagonist; OT, oxytocin; OTR, oxytocin receptor; TM, transmembrane helix; $V_{1a}R$, V_{1a} vasopressin receptor; $V_{1b}R$, V_{1b} vasopressin receptor; V_2R, V_2 vasopressin receptor; ACTH, adrenocorticotropic hormone.

bers of the neurohypophysial peptide hormone receptor family share certain sequence motifs and exhibit related pharmacologies (6–8). The hormone binding site of these receptors includes residues from the TM bundle (9, 10), ECL1 (11–13), and the N terminus (14–16).

Overall, the roles of residues located within the ECL domains of GPCRs are not well understood compared with residues in the TM domain. Nevertheless, extracellular residues are important for binding amine (17) and peptide ligands (18), binding allosteric modulators (19), human immunodeficiency virus coreceptor activity (20), switching agonist/antagonist properties (21), and modulating agonist-induced receptor internalization (22). For GPCRs in general, interest in the extracellular domains has focused on ECL2 in particular, because it projects into the binding crevice and there is direct evidence that its conformation changes upon receptor activation (23). The aim of this investigation was to provide a comprehensive pharmacological characterization defining the role of all the individual residues comprising the entire ECL2 domain of a peptide-GPCR. Systematic substitution of the $V_{1a}R$ by Ala generated a series of mutant receptors that were subsequently analyzed with respect to ligand binding (agonist/antagonist and peptide/non-peptide) and intracellular signaling. Our results establish that key residues located in ECL2 of the $V_{1a}R$ are required for normal receptor function, identifying Phe^{189}, Asp^{204}, Cys^{205}, Trp^{206}, Phe^{209}, and Tyr^{218} as essential for high affinity agonist binding and receptor activation.

EXPERIMENTAL PROCEDURES

Materials—AVP was purchased from Sigma. The cyclic peptide antagonist (CA) 1-(β-mercapto-β,β-cyclopentamethylenepropionic acid), 2-(*O*-methyl)tyrosine AVP ($d(CH_2)_5Tyr(Me)^2AVP$) and linear peptide antagonist (LA) phenylacetyl-D-$Tyr(Me)^2$ $Arg^6Tyr(NH_2)^9AVP$ were from Bachem (St. Helens, UK). SR 49059 was a gift from Sanofi Recherche (Toulouse, France). Cell culture media, buffers, and supplements were purchased from Invitrogen (Uxbridge, UK). Restriction enzymes DpnI, HindIII, KpnI, and EcoR1 were from New England Biolabs (Hitchin, UK) and Psp14601 was obtained from MBI Fermentas (Sunderland, UK).

Mutant Receptor Constructs—Mutation of the $V_{1a}R$ was made using a PCR approach as described previously (24). The mutant receptor constructs $[F189A]V_{1a}R$, $[S190A]V_{1a}R$, $[V191A]V_{1a}R$, $[I192A]V_{1a}R$, $[I194A]V_{1a}R$, $[V196A]V_{1a}R$, $[N197A]V_{1a}R$, $[G199A]V_{1a}R$, $[T200A]V_{1a}R$, $[K201A]V_{1a}R$, $[T202A]V_{1a}R$, $[Q203A]V_{1a}R$, $[C205A]V_{1a}R$, $[W206A]V_{1a}R$, $[A207G]V_{1a}R$, $[T208A]V_{1a}R$, $[F209A]V_{1a}R$, $[I210A]V_{1a}R$, and $[Q211A]V_{1a}R$ were engineered using the antisense oligonucleotides: 5′-GGC-GCG-GGT-ACC-CCA-GGG-CTG-GAT-G*AA*-C***G***-*TT*G-CCC-AGC-AGT-CTT-GGG-TTT-TAG-TG-C-CAT-TGT-TCA-CCT-CGA-TTT-CGA-TCA-CAG-AG**G**-**C**TA-TAA-AGT-ACT-GTG-G-3′, 5′-GGC-GCG-GGT-ACC-CCA-GGG-CTG-GAT-G*AA*-C***G***-*T*GC-CCA-GCA-GTC-TTG-GGT-TTT-AGT-GCC-ATT-GTT-CAC-CTC-GAT-TTC-GAT-CAC-AG**C**-GAA-TAT-AAA-GTA-CTG-TGG-3′, 5′-GGC-GCG-GGT-ACC-CCA-GGG-CTG-GAT-G*AA*-C***G***-*T*GC-CCA-GCA-GTC-TTG-GGT-TTT-AGT-GCC-ATT-GTT-CAC-CTC-GAT-TTC-GAT-C**G**C-AGA-GAA-TAT-AAA-GTA-CTG-TGG-3′, 5′-GGC-GCG-GGT-ACC-CCA-G-GG-CTG-GAT-G*AA*-C***G***-*TGC*-CCA-GCA-GTC-TTG-GG-T-TTT-AGT-GCC-ATT-GTT-CAC-CTC-GAT-TTC-G**GC**-CAC-AGA-GAA-TAT-AAA-GTA-CTG-TGG-3′, 5′-GGC-GCG-GGT-ACC-CCA-GGG-CTG-GAT-G*AA*-C***G***-*TGC*-C-CA-GCA-GTC-TTG-GGT-TTT-AGT-GCC-ATT-GTT-CA-C-CTC-G**GC**-TTC-GAT-ACA-GAG-3′, 5′-GGC-GCG-GG-T-ACC-CCA-GGG-CTG-GAT-G*AA*-C***G***-*TGC*-CCA-GCA-GTC-TTG-GGT-TTT-AGT-CCC-ATT-GTT-C**G**C-CTC-G-AT-TTCG-3′, 5′-GGC-GCG-GGT-ACC-CCA-GGG-CTG-GAT-G*AA*-C***G***-*T*GC-CCA-GCA-GTC-TTG-GGT-TTT-A-GT-GCC-ATT-G**GC**-ACC-TCG-ATT-TCG-3′, 5′-GGC-GC-G-GGT-ACC-CCA-GGG-CTG-GAT-G*AA*-C***G***-*T*CC-AGC-AGT-CTT-GGG-TTT-TAG-TG**G**-CAT-TGT-TCA-CC-3′, 5′-GGC-GCG-GGT-ACC-CCA-GGG-CTG-GAT-G*AA*-C***G***-*T*-*T*GC-CCA-GCA-GTC-TTG-GGT-TTT-AG**C**-GCC-ATT-GTT-CAC-C-3′, 5′-GGC-GCG-GGT-ACC-CCA-GGG-CT-G-GAT-G*AA*-C***G***-*T*GC-CCA-GCA-GTC-TTG-GGT-T**GC**-AGT-GCC-ATT-G-3′, 5′-GGC-GCG-GGT-ACC-CCA-GG-G-CTG-GAT-G*AA*-C***G***-*T*GC-CCA-GCA-GTC-TTG-GG**C**-TTT-AGT-GCC-3′, 5′-GGC-GCG-GGT-ACC-CCA-GGG-CTG-GAT-G*AA*-C***G***-*T*GC-CCA-GCA-GTC-T**GC**-GGT-T-TT-AGT-GC-3′, 5′-GGC-GCG-GGT-ACC-CCA-GGG-CT-G-GAT-G*AA*-C*C****G***-*TT*G-CCC-AG**G**-**C**GT-CTT-GGG-3′, 5′-GGC-GCG-GGT-ACC-CCA-GGG-CTG-GAT-G*AA*-C*GT*-*TGC*-C**GC**-GCA-GTC-TTG-GG-3′, 5′-GGC-GCG-GGT-ACC-CCA-GGG-CTG-GAT-G*AA*-C***G***-*T***C**C-CCA-GCA-GTC-3′, 5′-GGC-GCG-GGT-ACC-CCA-GGG-CTG-GAT-GAA-CG**C**-TGC-CCA-GC-3′, 5′-GGC-GCG-GGT-ACC-CCA-GGG-CTG-GAT-G**GC**-*C*GT-T*GC*-CCA-GC-3′, 5′-GGC-GCG-GGT-ACC-CCA-GGG-CTG-G**GC**-*GAA-CGT-T*GC-CCA-GC-3′, and 5′-GGC-GCG-GGT-ACC-CCA-GGG-C**GC**-GAT-G*AA*-C***G***-*T*GC-CCA-GC-3′, respectively. Each primer contained base changes for the Ala mutation (shown in bold) plus base changes to create a silent Psp1406I restriction site for diagnostic purposes where possible (shown in italics, with base changes in bold) and a unique KpnI restriction site (underlined) for subcloning. The sense primer was 5′-CGA-CTC-ACT-AT-A-GGG-AGA-CCC-AAG-CTT-3′ which contained a HindIII site (underlined) for subcloning. The constructs $[P212A]V_{1a}R$, $[W213A]V_{1a}R$, $[G214A]V_{1a}R$, $[T215]V_{1a}R$, $[R216A]V_{1a}R$, $[A217G]V_{1a}R$, and $[Y218A]V_{1a}R$ were engineered using the QuikChange site-directed mutagenesis kit (Stratagene, Cambridge, UK) following the manufacturer's instructions. The antisense primers were: 5′-CG**G**-GTA-C**GC**-CAG-G**C**C-TGG-ATG-AAC-G-3′, 5′-GCG-**C**GT-ACC-GG**C**-GGG-CTG-GAT-GAA-CG-3′, 5′-GGC-GCG-GGT-A**GC**-CCA-GGG-CTG-G-3′, 5′-CAC-GTA-GGC-GC**G**-GG**C**-AGC-CCA-GGG-C-3′, 5′-GGT-CAC-GTA-GGC-G**GC**-CGT-ACC-C-3′, 5′-GGT-CAC-GTA-G**C**C-GCG-**C**GT-ACC-C-3′, and 5′-GGT-CAT-CCA-G-GT-CAC-G**GC**-GGC-GCG-*GGT*-***C****CC*-CC-3′ respectively. The primers contained base changes (in bold) to incorporate point mutations and to ablate a KpnI site (underlined, base change in bold) for screening mutants. The sense primers were complementary to the antisense primers cited above. All receptor constructs were confirmed by automated fluorescent sequencing (University of Birmingham, Birmingham, UK).

Cell Culture and Transfection—HEK 293T cells were routinely cultured in Dulbecco's modified Eagle's medium supplemented with 10% (v/v) fetal calf serum in humidified 5% (v/v) CO_2 in air at 37 °C. Cells were seeded at a density of ~5×10^5 cells/100-mm dish and transfected after 48 h using a calcium phosphate precipitation protocol with 10 μg of DNA/dish (10).

Radioligand Binding Assays—A washed cell membrane preparation of HEK 293T cells, transfected with the appropriate receptor construct, was prepared as previously described (24), and the protein concentration was determined using the BCA protein assay kit (Pierce) using bovine serum albumin as standard. Radioligand binding assays were performed as previously described (25) using either the natural agonist [Phe^3-3,4,5-^{3}H]AVP (0.5–1.5 nM), (64.2 Ci/mmol, PerkinElmer Life Sciences), or the V_{1a}R-selective peptide antagonist phenylacetyl-D-Tyr(Me)^{2}Arg^6(3,4^{3}H-Pro)(3,5^{3}H-Tyr)^9NH_2-AVP (0.5–1.0 nM), (22 Ci/mmol, custom synthesis Pheonix Pharmaceuticals, Inc., Belmont, CA) (26) as tracer ligand. Binding data were analyzed by non-linear regression to fit theoretical Langmuir binding isotherms to the experimental data using Prism (GraphPad, San Diego, CA). Individual IC_{50} values obtained for competing ligands were corrected for radioligand occupancy as described (27) using the radioligand affinity (K_d) experimentally determined for each construct.

Determination of Cell-surface Expression Using Enzyme-linked Immunosorbent Assay—All receptor constructs incorporated an hemagglutinin epitope tag in the N terminus, which enabled cell-surface expression to be determined by enzyme-linked immunosorbent assay as described previously (28). Results were normalized against a wild-type control processed in parallel. Non-transfected cells were used to determine background. All experiments were performed in quadruplicate.

AVP-induced Inositol Phosphates Production—HEK 293T cells were seeded at a density of 2.5×10^5 cells/well in poly-D-lysine-coated 12-well plates and transfected after 24 h using Transfast™ (Promega, Madison, WI). AVP-induced accumulation of inositol phosphates (InsPs) was assayed as described previously (29). Briefly, following prelabeling of transfected cells with 2 μCi/ml myo-[2-^{3}H]inositol (22.0 Ci/mmol, PerkinElmer Life Sciences) in inositol-free Dulbecco's modified Eagle's medium containing 1% (v/v) fetal calf serum, a mixed fraction containing mono-, bis-, and trisphosphates (InsP-$InsP_3$) was collected following stimulation by AVP, at the concentrations indicated, in the presence of 10 mM LiCl.

RESULTS

Functional Importance of Individual Residues in ECL2 of the $V_{1a}R$—The individual residues comprising ECL2 of the V_{1a}R, plus the residues at the extracellular boundary of TMV, are presented in Fig. 1. Overall, this segment of the extracellular face of the V_{1a}R encompassed 30 residues, from Phe^{189} to Tyr^{218} inclusive. To assess the importance of these residues in V_{1a}R function, each residue was substituted individually by Ala (Ala^{207} and Ala^{217} were substituted by Gly) and then pharmacologically characterized using the natural agonist AVP and three structural classes of antagonist: (i) cyclic peptide antagonist (CA), [d(CH_2)$_5$Tyr(Me)^2]AVP, (30); (ii) linear peptide antagonist (LA), [phenylacetyl-D-Tyr(Me)^{2}Arg^{6}Tyr(NH_2)^9]AVP); and (iii), nonpeptide antagonist (SR 49059) (31). The K_d values are presented in Table 1, corrected for radioligand occupancy. The majority of mutant receptors exhibited wild-type pharmacology. Consequently, [S190A]V_{1a}R, [V191A]V_{1a}R, [I192A]V_{1a}R, [E193A]V_{1a}R, [I194A]V_{1a}R, [E195A]V_{1a}R, [V196A]V_{1a}R, [N197A]V_{1a}R, [G199A]V_{1a}R, [T200A]V_{1a}R, [K201A]V_{1a}R, [T202A]V_{1a}R, [Q203A]V_{1a}R, [A207G]V_{1a}R, [T208A]V_{1a}R, [I210A]V_{1a}R, [Q211A]V_{1a}R, [P212A]V_{1a}R, [W213A]V_{1a}R, [G214A]V_{1a}R, [T215A]V_{1a}R, [R216A]V_{1a}R, and [A217G]V_{1a}R had only a slight effect on the binding of the agonist AVP and the three different classes of antagonist (Table 1), indicating that the receptor protein was folded appropriately. The wild-type V_{1a}R and these mutant receptors were all expressed at the same level of 1–2 pmol/mg of protein. Furthermore, the intracellular signaling capability of these mutants was also essentially wild type (Table 2), consistent with the wild-type ligand binding profile of these receptor constructs.

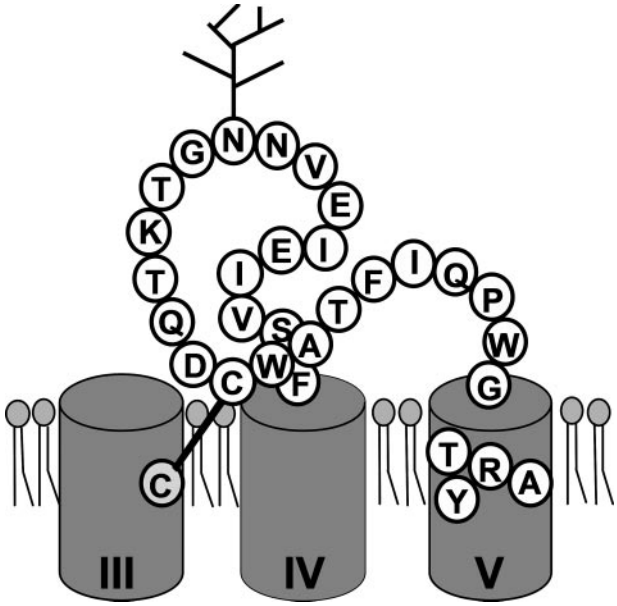

FIGURE 1. **Schematic diagram of ECL2 of the V_{1a}R.** The tops of TMIII–TMV are shown as *dark gray cylinders* and numbered accordingly. Residues investigated in this study are shown as *white circles*. The Cys (*light gray circle*) at the top of TMIII is not part of this study and is included to show the position of the conserved disulfide bond (*black line*) between ECL2 and TMIII. The branched structure indicates an *N*-glycosylation site previously shown experimentally to be utilized (42).

In marked contrast, [F189A]V_{1a}R, [C205A]V_{1a}R, [W206A]V_{1a}R, [F209A]V_{1a}R, and [Y218A]V_{1a}R exhibited severely impaired agonist binding, with AVP affinity decreasing ~2000-fold for [W206A]V_{1a}R, [Y218A]V_{1a}R, and ~200-fold for [F209A]V_{1a}R, compared with wild type (Fig. 2). The affinity of the three classes of antagonist remained essentially wild type for [W206A]V_{1a}R and [F209A]V_{1a}R (Table 1), indicating that the mutant receptor proteins were folded appropriately. It was noted, however, that the affinity of CA for [F209A]V_{1a}R was decreased 8-fold relative to wild type (Table 1). It should be noted that we recently reported in a separate study (28) that substitution of Asp^{204} by Ala disrupted agonist binding and intracellular signaling. Consequently, these data will not be discussed in detail here; however, data for [D204A]V_{1a}R are cited

TABLE 1

Pharmacological profile of ECL2 mutant V_{1a}Rs

Mutant V_{1a}Rs were expressed in HEK 293T cells and characterized pharmacologically. Dissociation constants (K_d) were calculated from IC_{50} values and corrected for radioligand occupancy as described under "Experimental Procedures." Data shown are the mean ± S.E. ($n = 3$) of three replicates. CA = cyclic peptide antagonist, LA = linear peptide antagonist, SR 49059 = nonpeptide antagonist.

Receptor	Binding affinities, K_d			
	AVP	CA	LA	SR 49059
		nM		
Wild-type V_{1a}R	1.0 ± 0.1	0.7 ± 0.3	0.5 ± 0.1	1.9 ± 0.3
F189A	No binding		No binding	
S190A	2.75 ± 1.01	1.95 ± 0.77	0.28 ± 0.06	1.98 ± 0.46
V191A	1.91 ± 0.91	1.61 ± 0.36	0.22 ± 0.03	1.35 ± 0.13
I192A	2.51 ± 0.35	2.50 ± 0.74	1.10 ± 0.68	2.84 ± 0.86
E193A[a]	1.53 ± 0.21	0.93 ± 0.25	1.02 ± 0.10	0.28 ± 0.02
I194A	0.75 ± 0.44	1.55 ± 0.18	1.55 ± 0.18	1.40 ± 0.45
E195A[a]	0.89 ± 0.03	0.63 ± 0.08	0.18 ± 0.10	3.39 ± 0.54
V196A	2.20 ± 0.48	1.28 ± 0.42	1.07 ± 0.31	1.61 ± 0.49
N197A	2.06 ± 0.38	1.84 ± 0.35	2.24 ± 0.59	3.28 ± 0.71
N198Q[b]	0.90 ± 0.10	0.50 ± 0.10	0.50 ± 0.10	1.60 ± 0.20
G199A	1.85 ± 0.43	2.64 ± 0.44	0.50 ± 0.08	2.50 ± 1.30
T200A	2.34 ± 0.40	0.55 ± 0.26	2.37 ± 1.29	1.48 ± 0.62
K201A	1.42 ± 0.32	0.44 ± 0.36	0.70 ± 0.30	1.35 ± 0.27
T202A	1.76 ± 0.08	1.72 ± 0.19	2.00 ± 0.96	2.53 ± 0.52
Q203A	1.67 ± 0.33	1.89 ± 0.44	1.51 ± 0.54	2.26 ± 0.84
D204A[a]	2300 ± 240	2.00 ± 0.4	10.0 ± 3.4	1.3 ± 1.2
C205A	No binding		No binding	
W206A	1431 ± 344	2.03 ± 0.51	0.32 ± 0.06	1.04 ± 0.26
A207G	1.64 ± 0.11	1.20 ± 0.35	0.45 ± 0.13	1.05 ± 0.05
T208A	1.09 ± 0.17	1.85 ± 0.30	0.70 ± 0.12	1.84 ± 0.16
F209A	212 ± 72	5.90 ± 1.13	0.10 ± 0.02	1.22 ± 0.21
I210A	1.30 ± 0.12	1.62 ± 0.59	1.76 ± 0.69	2.48 ± 0.28
Q211A	1.95 ± 0.28	0.94 ± 0.15	0.88 ± 0.32	1.47 ± 0.31
P212A	1.03 ± 0.36	0.75 ± 0.07	0.93 ± 0.31	1.16 ± 0.21
W213A	1.92 ± 0.86	2.18 ± 0.40	0.92 ± 0.23	2.96 ± 1.51
G214A	1.50 ± 0.09	1.16 ± 0.28	0.29 ± 0.06	1.33 ± 0.41
T215A	0.92 ± 0.28	0.70 ± 0.16	0.51 ± 0.09	1.84 ± 0.52
R216A[a]	0.80 ± 0.13	0.44 ± 0.05	0.46 ± 0.10	0.93 ± 0.17
A217G	2.49 ± 0.30	2.24 ± 0.06	1.64 ± 0.30	3.99 ± 1.05
Y218A	1954 ± 525	1478 ± 357	0.93 ± 0.20	96.1 ± 20.8

[a] Data from Ref. 28.
[b] Data from Ref. 42.

TABLE 2

Intracellular signaling by ECL2 mutant V_{1a}Rs

EC_{50} and E_{max} values of AVP-induced accumulation of InsP-$InsP_3$ in cells expressing wild-type (WT) and mutant receptors are shown. Values shown are the mean ± S.E. of three separate experiments performed in triplicate. Basal values (mean ± S.E.) were 1228 ± 146, 1064 ± 93, 1197 ± 139, 1043 ± 28, 1346 ± 135, 891 ± 170, 1053 ± 115, 1009 ± 188, 929 ± 187, 1219 ± 74, 1043 ± 25, 1213 ± 255, 911 ± 24, 1250 ± 143, 893 ± 93, 1554 ± 279, 973 ± 146, 1073 ± 100, 788 ± 239, 1213 ± 240, 860 ± 23, 969 ± 59, 1246 ± 14, 1246 ± 14, 1684 ± 347, 1128 ± 203, 831 ± 132, 1154 ± 153, 953 ± 186, 1083 ± 162, and 864 ± 11 dpm for wild-type V_{1a}R, [F189A]V_{1a}R, [S190A]V_{1a}R, [V191A]V_{1a}R, [I192A]V_{1a}R, [E193A]V_{1a}R, [I194A]V_{1a}R, [E195A]V_{1a}R, [V196A]V_{1a}R, [N197A]V_{1a}R, [N198Q]V_{1a}R, [G199A]V_{1a}R, [T200A]V_{1a}R, [K201A]V_{1a}R, [T202A]V_{1a}R, [Q203A]V_{1a}R, [D204A]V_{1a}R, [C205A]V_{1a}R, [W206A]V_{1a}R, [A207G]V_{1a}R, [T208A]V_{1a}R, [F209A]V_{1a}R, [I210A]V_{1a}R, [Q211A]V_{1a}R, [P212A]V_{1a}R, [W213A]V_{1a}R, [G214A]V_{1a}R, [T215]V_{1a}R, [R216A]V_{1a}R, [A217G]V_{1a}R, and [Y218A]V_{1a}R, respectively. None of the mutant receptors displayed constitutive activity.

Receptor construct	AVP-induced IP-IP_3 accumulation	
	EC_{50}	E_{max}
	nM	*-Fold*
Wild-type V_{1a}R	1.18 ± 0.16	5.52 ± 0.26
F189A	146.89 ± 14.02	1.71 ± 0.04
S190A	2.39 ± 0.40	6.11 ± 1.03
V191A	2.49 ± 1.07	7.12 ± 0.43
I192A	1.45 ± 0.08	5.16 ± 1.43
E193A	0.30 ± 0.12	4.98 ± 0.12
I194A	3.20 ± 1.39	5.64 ± 1.23
E195A	1.01 ± 0.13	7.88 ± 0.65
V196A	1.05 ± 0.17	4.60 ± 1.10
N197A	1.16 ± 0.05	6.51 ± 0.52
G199A	1.14 ± 0.62	3.98 ± 0.02
T200A	1.55 ± 0.52	3.92 ± 0.92
K201A	1.56 ± 0.32	7.95 ± 0.16
T202A	1.56 ± 0.32	4.72 ± 0.19
Q203A	1.18 ± 0.11	7.26 ± 1.47
D204A	7.00 ± 1.30	4.80 ± 0.50
C205A	NS[a]	NS
W206A	20.24 ± 7.57	4.56 ± 0.56
A207G	0.83 ± 0.12	9.88 ± 3.76
T208A	1.40 ± 0.38	5.85 ± 2.30
F209A	13.75 ± 5.83	6.21 ± 0.86
I210A	0.87 ± 0.13	7.17 ± 0.96
Q211A	0.46 ± 0.22	5.18 ± 0.59
P212A	1.41 ± 0.38	3.47 ± 1.12
W213A	1.51 ± 0.18	5.84 ± 1.67
G214A	1.16 ± 0.34	6.75 ± 1.36
T215A	0.57 ± 0.37	6.72 ± 1.69
R216A	0.30 ± 0.03	6.46 ± 0.12
A217G	0.88 ± 0.26	7.23 ± 2.02
Y218A	39.31 ± 10.54	7.24 ± 1.08

[a] NS, no stimulation.

in Table 1 to provide a complete study. In addition to the marked decrease in AVP affinity noted above, [Y218A]V_{1a}R also had decreased affinity compared with wild type, for CA (2000-fold) and SR49059 (50-fold). However, LA binding to [Y218A]V_{1a}R was essentially wild type. The LA binding indicated that the overall fold of the receptor was appropriate and, furthermore, allowed quantification of ligand binding affinities to [Y218A]V_{1a}R using [^{3}H]LA as tracer (Table 1). Because neither of the radioligands available bound to [F189A]V_{1a}R nor [C205A]V_{1a}R within the practical concentration range for ligand binding assays, it was not possible to quantify the decrease in ligand affinity at these mutant receptors.

Role of Key Individual Residues in ECL2 of the V_{1a}R in Intracellular Signaling—Assaying AVP-induced accumulation of InsP-$InsP_3$ revealed that the ECL2 mutants [F189A]V_{1a}R, [C205A]V_{1a}R, [W206A]V_{1a}R, [F209A]V_{1a}R, and [Y218A]V_{1a}R all exhibited impaired intracellular signaling (Table 2), with the degree of perturbation being dependent on the locus of the mutation (Fig. 3). The severity of the impaired signaling could be divided into three groups: (i) [W206A]V_{1a}R, [F209A]V_{1a}R, and [Y218A]V_{1a}R had EC_{50} values for AVP-induced accumulation of InsP-$InsP_3$ 20-fold, 14-fold, and 39-fold, respectively, greater than wild-type V_{1a}R; (ii) [F189A]V_{1a}R exhibited an EC_{50} value ~150-fold greater than wild-type V_{1a}R; and (iii) [C205A]V_{1a}R was incapable of initiating a InsP-$InsP_3$ response when challenged by a high AVP concentration (1 μM). None of the mutant receptors displayed constitutive activity.

Given that the mutant receptors [F189A]V_{1a}R, [C205A]V_{1a}R, [W206A]V_{1a}R, [F209A]V_{1a}R, and [Y218A]V_{1a}R had impaired ligand binding and intracellular signaling, cell-surface expression of these constructs was determined (Fig. 4). Cell-surface expression of [W206A]V_{1a}R was wild type, whereas the surface expression of [F189A]V_{1a}R, [F209A]V_{1a}R, and [Y218A]V_{1a}R was 60–80% of wild type. The surface expression of [C205A]V_{1a}R was only 40% of wild-type and was the lowest of all the engineered constructs.

DISCUSSION

The ECL2 domain of bRho forms a β-hairpin that plunges down into the TM bundle, forming a lid over the bound retinal, which shields it from the extracellular milieu. This protein fold positions residues in the second β-strand (β4) of this ECL2 hairpin structure in close proximity to the chromophore. Consequently, Glu^{181}, Gly^{188}, Ile^{189}, and Tyr^{191} of bRho all make contact with retinal (1). Given the unusual nature of the

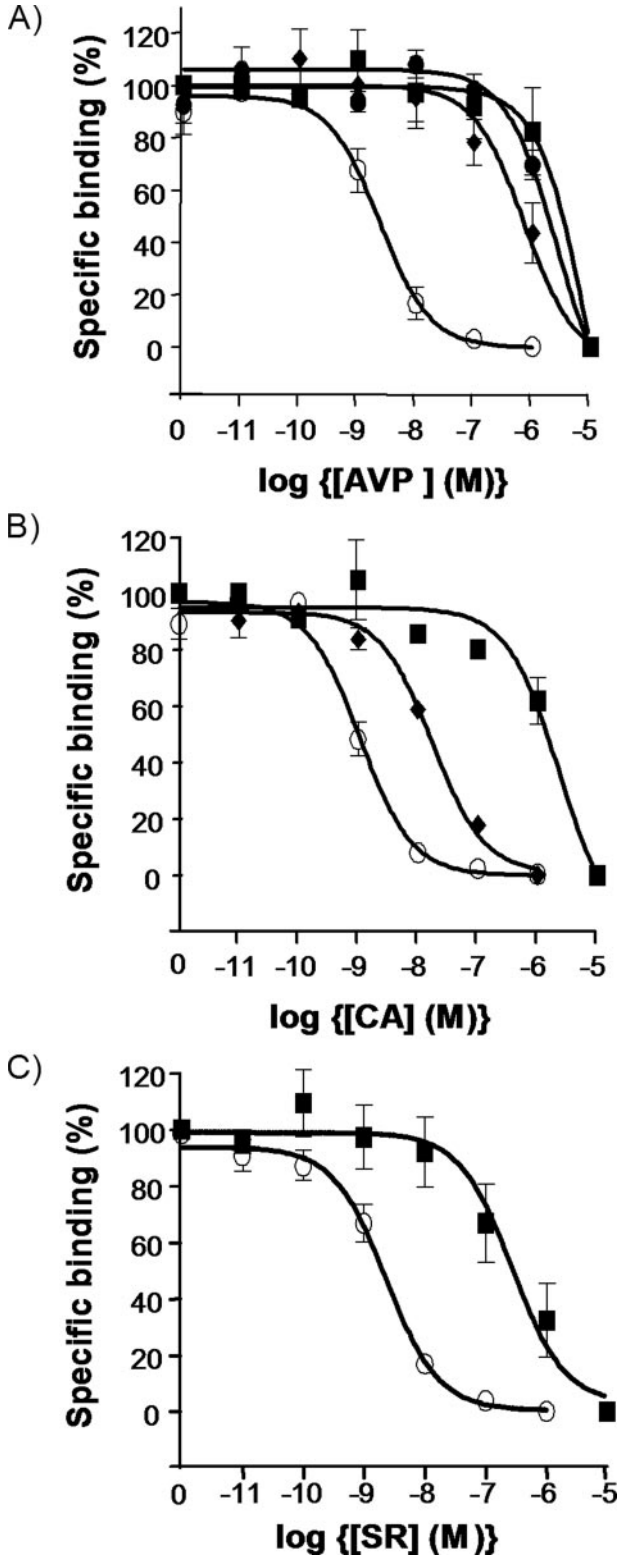

FIGURE 2. **Pharmacological characterization of ECL2 mutant receptors.** Radioligand binding assays were performed using a membrane preparation of HEK 293T cells transiently transfected with either: wild-type $V_{1a}R$ (○), [W206A]$V_{1a}R$ (●), [F209A]$V_{1a}R$ (◆), and [Y218A]$V_{1a}R$ (■) with the competing ligand being AVP (*A*), CA (*B*), or SR49059 (*C*). Data are the mean ± S.E. of three separate experiments each performed in triplicate using [^{3}H]AVP (0.5–1.5 nM) or [^{3}H]LA (0.5–1.0 nM) as tracer. Values are expressed as percent specific binding where nonspecific binding was defined by d(CH$_2$)$_5$Tyr(Me)^{2}AVP (1 μM) or LA (1 μM). A theoretical Langmuir binding isotherm has been fitted to the experimental data as described under "Experimental Procedures."

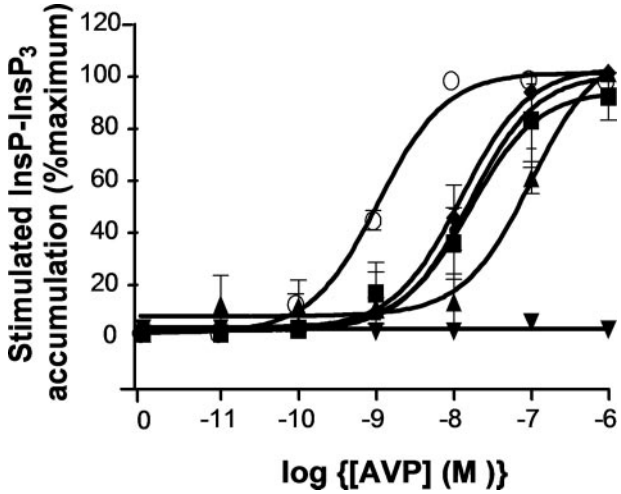

FIGURE 3. **Intracellular signaling by ECL2 mutant receptors.** AVP-induced accumulation of inositol mono-, bis-, and trisphosphates in HEK 293T cells transiently transfected with: wild-type $V_{1a}R$ (○), [F189A]$V_{1a}R$ (▲), [C205A]$V_{1a}R$ (▼), [W206A]$V_{1a}R$ (●), [F209A]$V_{1a}R$ (◆), and [Y218A]$V_{1a}R$ (■). Data are the mean ± S.E. of three separate experiments each performed in triplicate. Values are stimulation induced by AVP at the stated concentrations expressed as percent maximum.

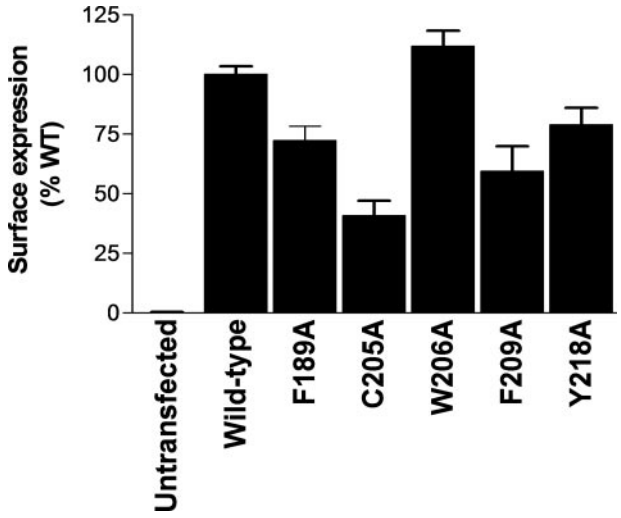

FIGURE 4. **Cell-surface expression of ECL2 mutant receptors.** The cell-surface expression of mutant receptors was determined by enzyme-linked immunosorbent assay as described in "Experimental Procedures." Results were normalized against a wild-type control processed in parallel. Non-transfected cells were used to determine background. All experiments were performed three times in triplicate.

covalently bound ligand in bRho, the variation in sequence and length of ECL2 within Family A GPCRs, and the requirement for reversible ligand access from the extracellular medium, it is perhaps possible that this β-hairpin fold is a unique feature of opsins. Indeed, the two-dimensional nuclear magnetic resonance structure of some synthetic ECL2 peptides has resulted in GPCR models that incorporate a different conformation. For example, it has been proposed that ECL2 of the thromboxane A_2 receptor contains two β-turns and extends away from the TM bundle (32). Alternatively, a helical conformation preceding the conserved Cys, or central to the ECL2 loop, was suggested for the κ-opioid receptor (33) and the neurokinin-1 receptor (34, 35), respectively. However, using the substituted-cysteine accessibility method to identify residues contributing

to the water-accessible binding site crevice of the D_2 dopamine receptor (D_2R), Shi and Javitch concluded that the ECL2 loop of the D_2R adopted a similar conformation as the corresponding loop in bRho (4). In addition, this conclusion is consistent with ECL2 site-directed mutagenesis data for other Family A GPCRs (reviewed in Ref. 17).

The aim of this study was to systematically define the role of the individual residues that comprise the ECL2 domain of the $V_{1a}R$. The majority of these mutant receptor constructs, 24 in total, had essentially wild-type ligand binding and intracellular signaling characteristics, indicating that these residues were not important for normal receptor function. In contrast, substitution of Cys^{205} ablated both ligand binding and signaling. This Cys is part of the disulfide bond between ECL2 and the top of TMIII ($Cys^{3.25}$),[6] which is conserved in nearly all Family A GPCRs, and contributes to structural integrity of the receptor. Consistent with this structural role, cell-surface expression of [C205A]$V_{1a}R$ was only 40% of wild type. Receptor function was also disrupted when the corresponding Cys was mutated in bRho (36), M3 muscarinic acetylcholine receptor (37), β_2-adrenergic receptor (β_2-AR) (38), NK_1 receptor (39), and the gonadotropin-releasing hormone receptor (40).

There are a total of five aromatic residues within the extracellular segment of the $V_{1a}R$ investigated in this study, Phe^{189}, Trp^{206}, Phe^{209}, Trp^{213}, and Tyr^{218}. All five residues are highly conserved throughout members of the vertebrate neurohypophysial hormone sub-family of GPCRs cloned to date (Fig. 5). Furthermore, residues Trp^{206}, Phe^{209}, Trp^{213}, and Tyr^{218} are part of a sequence motif, DCWA*X*F*XX*PWG*X*(R/K)AY, which is highly conserved throughout this sub-family of GPCRs but is not a feature of Family A GPCRs in general. This family-specific conservation, plus the extracellular location of the motif in the receptor architecture, led to the hypothesis that residues in this motif may be candidates for ligand recognition (5, 41). Consistent with this hypothesis, we show in the current study that mutation of the aromatic residues Trp^{206}, Phe^{209}, or Tyr^{218} (shown underlined in the motif DC**W**A*X***F***XX*PWG*X*(R/K)A**Y**) resulted in decreased affinity for agonist (Table 1) and impaired intracellular signaling (Table 2). This loss of AVP binding was not due to gross aberrant assembly of the mutant receptors, because the binding of at least one antagonist was wild type. Disruption of receptor function was not due to poor expression of the mutant receptors, because cell-surface expression of [W206A]$V_{1a}R$, [F209A]$V_{1a}R$, and [Y218A]$V_{1a}R$ was 60–100% of wild type (Fig. 4), and we have shown previously that a mutant receptor expressed at only 50% of wild-type $V_{1a}R$ exhibited wild-type signaling (28). In common with Trp^{206}, Phe^{209}, and Tyr^{218}, the residue Trp^{213} is also part of the DCWA*X*F*XX*-P**W**G*X*(R/K)AY motif (shown underlined) and is highly conserved in neurohypophysial hormone receptors cloned to date, with the single exception of the vasotocin receptor from bull frog, in which Lys replaces the Trp. However, despite this high degree of conservation, Trp^{213} is not important for receptor function, because [W213A]$V_{1a}R$ exhibited essentially wild-type ligand binding and signaling.

[6] Residues in the TMs are referred to by residue number and the nomenclature of Ballesteros and Weinstein (43).

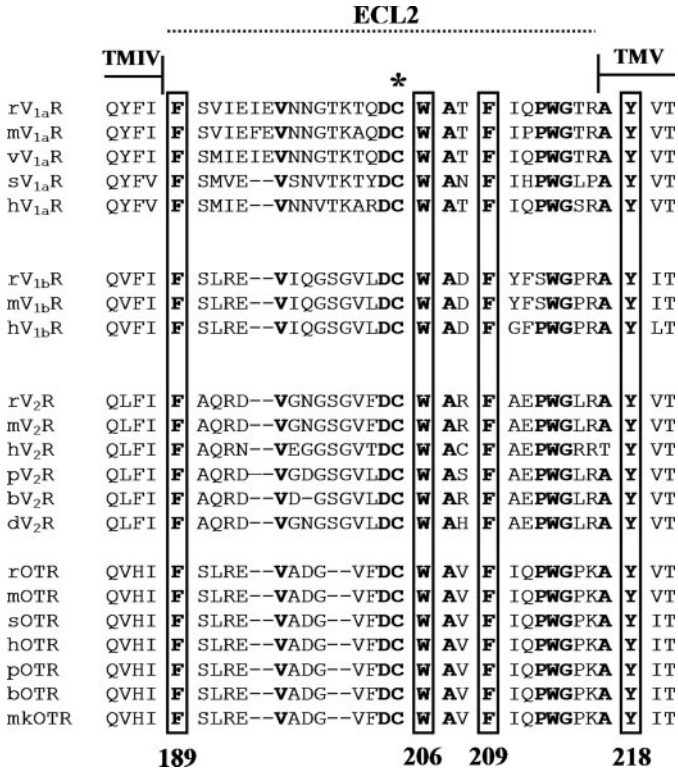

FIGURE 5. **Comparison of the ECL2 sequence of neurohypophysial hormone receptors cloned from different species.** The sequences of the ECL2 domain of the $V_{1a}R$, $V_{1b}R$, V_2R, and OTR from different species have been aligned. The species of origin is indicated by a *single letter code* preceding the receptor subtype: *r*, rat; *m*, mouse; *v*, vole; *s*, sheep; *h*, human; *p*, pig; *b*, cow; *d*, dog; *mk*, rhesus monkey. ECL2 residues that are highly conserved throughout the neurohypophysial hormone receptor family are shown in *bold*. The highly conserved aromatic residues within ECL2, shown to be functionally important in this study, are *boxed* and *numbered* according to the $rV_{1a}R$ sequence. Sequences cited were obtained from SwissProt and GenEMBL. The Cys in ECL2 which forms part of the disulfide bond conserved in Family A GPCRs is indicated by an *asterisk*.

Conserved residues within the TM bundle were used to establish a universal residue nomenclature system (43). It is difficult to directly compare ECL2 residues from different GPCRs, because there is a lack of sequence conservation and the loop length varies between receptors. However, ECL2 contains a highly conserved Cys, which is one half of the disulfide bond conserved in the majority of Family A GPCRs. This disulfide bond will spatially constrain relative movement between ECL2 and TMIII and therefore provide a point of reference for comparison between different GPCRs. We propose an indexing method for comparing aligned ECL2 residues in different GPCRs in which the conserved Cys is the reference point and other residues are indexed relative to this position. For example, for the rat $V_{1a}R$ (Fig. 5), the residue preceding the conserved Cys is $Asp^{(C-1)}$ and the residue following the Cys is $Trp^{(C+1)}$.

$Trp^{206(C+1)}$ and $Phe^{209(C+4)}$ in the $V_{1a}R$ correspond to $Gly^{188(C+1)}$ and $Tyr^{191(C+4)}$ in bRho. In the bRho crystal structure, $Gly^{188(C+1)}$ and $Tyr^{191(C+4)}$ are in the β4 strand of the ECL2 hairpin and come within 5 Å of the retinal to form part of the chromophore binding pocket (1, 44). Consequently, assuming that the tertiary fold of ECL2 in the $V_{1a}R$ is similar to that of ECL2 in bRho, then $Trp^{206(C+1)}$ and $Phe^{209(C+4)}$ will be

directed down into the binding cavity within the helical bundle. Such an orientation of these residues would be entirely consistent with the disruption of ligand binding and signaling observed for [W206A]V_{1a}R and [F209A]V_{1a}R. It is noteworthy that C+1 and C+4 residues in this "β4 strand segment" of ECL2 can also be important for ligand binding to amine-GPCRs. Indeed, $Phe^{209(C+4)}$ is part of the Cys-*X*-*X*-*X*-Ar motif (where Ar is an aromatic residue) that is well conserved in both peptide-GPCRs (59%) and amine-GPCRs (17%). In addition, $Gln^{189(C+1)}$ of the 5-HT_{1D} receptor, corresponding to $Trp^{206(C+1)}$ of the V_{1a}R, contributes to the subtype selectivity of ketanserin (45), and $Gln^{177(C+1)}$ is part of a triad of ECL2 residues responsible for α_{1A}AR *versus* α_{1B}AR pharmacology (46). In peptide-GPCRs, $Arg^{197(C+1)}$ of the cholecystokinin-1 receptor makes direct contact with $Tyr(SO_4)^2$ of cholecystokinin (47) and mutation of $Tyr^{190(C+4)}$ in the CXCR4 chemokine receptor, resulted in impaired signaling (48).

$Tyr^{218(5.38)}$ at the extracellular boundary of TMV is absolutely conserved throughout the neurohypophysial peptide hormone receptor sub-family of GPCRs and is part of the same conserved sequence motif (DCWA*X*F*XX*PWG*X*(R/K)A**Y**, shown underlined) as $Trp^{206(C+1)}$ and $Phe^{209(C+4)}$. Mutation of $Tyr^{218(5.38)}$ in the construct [Y218A]V_{1a}R disrupted both ligand binding and intracellular signaling suggesting that $Tyr^{218(5.38)}$ is orientated into the ligand binding site. For the D_2R, it has been shown that the corresponding residue $Phe^{5.38}$ points into the binding site crevice by using a substituted-cysteine accessibility method in conjunction with ligand protection (49). Likewise, mutation of $Tyr^{5.38}$ of the α_{1B}-adrenergic receptor also disrupted agonist binding and signaling (50). Our conclusion that $Tyr^{218(5.38)}$ orientates into the ligand binding crevice also provides a feasible mechanism for the naturally occurring "loss-of-function" mutation Y205C in the human V_2R (equivalent to Tyr^{218} in the V_{1a}R), which has been identified as a cause of nephrogenic diabetes insipidus in some families (51).

The conserved residues in ECL2 corresponding to $Val^{196(C-9)}$ plus $Ala^{211(C+2)}$, $Pro^{212(C+7)}$, $Gly^{214(C+9)}$, $Arg^{216(C+11)}$, and $Ala^{217(C+12)}$ (shown underlined in DCW**A***X*F*XX***P**W**G***X*(**R/K**)**A**Y) are present in all vertebrate AVP/OT receptors cloned to date (Fig. 5), with the exception of only the rodent V_{1b}R ($Pro^{(C+7)} \rightarrow$ Ser), the sheep V_{1a}R ($Arg^{(C+11)} \rightarrow$ Pro), and the human V_2R ($Ala^{(C+12)} \rightarrow$ Thr). Nevertheless, the mutant receptors [V196A]V_{1a}R, [A211G]V_{1a}R, [P212A]V_{1a}R, [G214A]V_{1a}R, [R216A]V_{1a}R, and [A217G]V_{1a}R were all near wild type with respect to binding agonist, three different classes of antagonist and intracellular signaling capability. Consequently, despite comprising a large part of a "signature motif" throughout the AVP/OT receptor family, these conserved ECL2 residues do not seem to have a role in receptor function.

Phe^{189} at the start of ECL2 is highly conserved throughout the neurohypophysial peptide hormone receptor family with the single exception of the cephalotocin receptor, found in octopus, where a Trp replaces the conserved Phe. This high level of conservation reflects functional importance, because [F189A]V_{1a}R exhibited a dramatic decrease in potency (~150-fold) of AVP-induced InsP signaling and severely disrupted ligand binding. The corresponding residue (Trp^{175}) in bRho packs against Phe^{203} at the top of TMV (corresponding to Tyr^{218} in the V_{1a}R) (52). It is likely that this interaction between the extreme ends of ECL2 is important for the orientation/stability of the ECL2 cap over the binding pocket, because both [F189A]V_{1a}R and [Y218A]V_{1a}R possessed disrupted ligand binding and signaling (this study) and [W175A]bRho exhibited impaired regeneration of the dark photoreceptive state following photoactivation (53). Although it is clear that the ECL2 domain can fulfill a range of functions in GPCRs in general, the details of its role are receptor-specific. Random saturation mutagenesis of ECL2 in the C5a receptor (C5aR) identified multiple mutations exhibiting constitutive activity, suggesting that in the wild-type receptor ECL2 stabilized the inactive C5aR (54). Likewise, for another glycoprotein-GPCR, the thyroid-stimulating hormone receptor, it has been reported that an interaction between ECL2 and TMVI constrains the receptor in an inactive state. Consequently, substitution of Ile^{568} in ECL2 of the thyroid-stimulating hormone receptor by a range of diverse residues (including the pathogenic mutant I568V) generates constitutive activity (55). In contrast, random mutagenesis of the M3 muscarinic acetylcholine receptor (M3R) identified several ECL2 residues important for stabilizing the active state of the M3R mAChR and furthermore, established that ECL2 residues were not important for agonist binding to M3R (56). In the current study, we have established that key residues provided by ECL2 of a small peptide-GPCR are important for agonist binding and receptor activation. Consequently, ECL2 is important for normal function of the C5aR, M3R, and V_{1a}R, but the role fulfilled by ECL2 is different for each of these receptors. These differences in the role of ECL2 probably reflect differences in the binding mode between large peptide ligand, amine ligand, and small peptide ligand, respectively.

The side chain of Asn^{198} is not available for inter-molecular or intra-molecular contacts, because it is modified by *N*-linked glycosylation. The carbohydrate is not required for ligand binding or intracellular signaling but does have a role in cell-surface expression (42). This post-translational modification has to be accommodated within the tertiary structure of ECL2. If ECL2 forms a plunging β-hairpin in V_{1a}R, similar to bRho, then the oligosaccharide chain must project from the helical bundle into the extracellular medium without steric clashes. Alternatively if the ECL2 domain extends into the extracellular milieu, then glycosylation of ECL2 may serve to stabilize this orientation. Although ECL2 in bRho is not glycosylated, such modification is not rare in GPCRs. Analyzing the sequences of 613 Family A GPCRs revealed that 32% possess at least one consensus *N*-glycosylation site (N*X*(S/T)) in ECL2. For the vast majority of these receptors (85%), the ECL2 *N*-glycosylation site is not located within the sequence corresponding to the β4-strand of bRho, *i.e.* not within the deeply buried β-strand of the ECL2 hairpin, thereby allowing the oligosaccharide to be accommodated more easily within the tertiary structure.

In conclusion, we have shown that key residues located in ECL2 of the V_{1a}R are required for normal receptor function, identifying Phe^{189}, Asp^{204}, Cys^{205}, Trp^{206}, Phe^{209}, and Tyr^{218} as essential for high affinity agonist binding and receptor activation. In addition, Tyr^{218} was also required for high affinity binding of CA and nonpeptide antagonist. Consistent with their fundamental role in receptor function, these residues are highly

conserved throughout the neurohypophysial hormone receptor sub-family of GPCRs.

Acknowledgment—We are grateful to Dr. Claudine Serradeil-Le Gal (Sanofi-Avantis Recherche & Développement, Toulouse, France) for providing a sample of SR 49059.

REFERENCES

1. Palczewski, K., Kumasaka, T., Hori, T., Behnke, C. A., Motoshima, H., Fox, B. A., Le Trong, I., Teller, D. C., Okada, T., Stenkamp, R. E., Yamamoto, M., and Miyano, M. (2000) *Science* **289,** 739–745
2. Li, J., Edwards, P. C., Burghammer, M., Villa, C., and Schertler, G. F. X. (2004) *J. Mol. Biol.* **343,** 1409–1438
3. Lu, Z. L., Saldanha, J. W., and Hulme, E. C. (2002) *Trends Pharmacol. Sci.* **23,** 140–146
4. Shi, L., and Javitch, J. A. (2004) *Proc. Natl. Acad. Sci. U. S. A.* **101,** 440–445
5. Thibonnier, M., Coles, P., Thibonnier, A., and Shoham, M. (2001) *Annu. Rev. Pharmacol. Toxicol.* **41,** 175–202
6. Gimpl, G., and Fahrenholz, F. (2001) *Physiol. Rev.* **81,** 629–683
7. Howl, J., and Wheatley, M. (1995) *Gen. Pharmacol.* **26,** 1143–1152
8. Hibert, M., Hoflack, J., Trumpp-Kallmeyer, S., Mouillac, B., Chini, B., Mahe, E., Cotte, N., Jard, S., Manning, M., and Barberis, C. (1999) *J. Recept. Signal Transduct. Res.* **19,** 589–596
9. Mouillac, B., Chini, B., Balestre, M.-N., Elands, J., Trump-Kallmeyer, S., Hoflack, J., Hibert, M., Jard, S., and Barberis, C. (1995) *J. Biol. Chem.* **270,** 25771–25777
10. Hawtin, S. R., Ha, S. N., Pettibone, D. J., and Wheatley, M. (2005) *FEBS Lett.* **579,** 349–356
11. Howl, J., and Wheatley, M. (1996) *Biochem. J.* **317,** 577–582
12. Kojro, E., Eich, P., Gimpl, G., and Fahrenholz, F. (1993) *Biochemistry* **32,** 13537–13544
13. Chini, B., Mouillac, B., Ala, Y., Balestre, M.-N., Trump-Kallmeyer, S., Hoflack, J., Elands, J., Hibert, M., Manning, M., Jard, S., and Barberis, C. (1995) *EMBO J.* **14,** 2176–2182
14. Hawtin, S. R., Wesley, V. J., Parslow, R. A., Simms, J., Miles, A., McEwan, K., and Wheatley, M. (2002) *Mol. Endocrinol.* **16,** 600–609
15. Hawtin, S. R., Wesley, V. J., Simms, J., Argent, C. C. H., Latif, K., and Wheatley, M. (2005) *Mol. Endocrinol.* **19,** 2871–2881
16. Wesley, V. J., Hawtin, S. R., Howard, H. C., and Wheatley, M. (2002) *Biochemistry* **41,** 5086–5092
17. Shi, L., and Javitch, J. A. (2002) *Annu. Rev. Pharmacol. Toxicol.* **42,** 437–467
18. Ding, X. Q., Pinon, D. I., Furse, K. E., Lybrand, T. P., and Miller, L. J. (2002) *Mol. Pharmacol.* **61,** 1041–1052
19. Gnagey, A. L., Seidenberg, M., and Ellis, J. (1999) *Mol. Pharmacol.* **56,** 1245–1253
20. Brelot, A., Heveker, N., Montes, M., and Alizon, M. (2000) *J. Biol. Chem.* **275,** 23736–23744
21. Ott, T. R., Troskie, B. E., Roeske, R. W., Illing, N., Flanagan, C. A., and Millar, R. P. (2002) *Mol. Endocrinol.* **10,** 1079–1088
22. Li, S., Liu, X., Min, L., and Ascoli, M. (2001) *J. Biol. Chem.* **276,** 7968–7973
23. Banères, J.-L., Mesnier, D., Martin, A., Joubert, L., Dumuis, A., and Bockaert, J. (2005) *J. Biol. Chem.* **280,** 20253–20260
24. Hawtin, S. R., Tobin, A., Patel, S., and Wheatley, M. (2001) *J. Biol. Chem.* **276,** 38139–38146
25. Howl, J., Langel, Ü., Hawtin, S. R., Valkna, A., Yarwood, N. J., Saar, K., and Wheatley, M. (1997) *FASEB J.* **11,** 582–590
26. Schmidt, A., Audigier, S., Barberis, C., Jard, S., Manning, M., Kolodziejczyk, A. S., and Sawyer, W. H. (1991) *FEBS Letts.* **282,** 77–81
27. Cheng, Y., and Prusoff, W. H. (1973) *Biochem. Pharmacol.* **22,** 3099–3108
28. Hawtin, S. R., Simms, J., Conner, M., Lawson, Z., Parslow, R. A., Trim, J., Sheppard, A., and Wheatley, M. (2006) *J. Biol. Chem.* **281,** 38478–38488
29. Hawtin, S. R., Wesley, V. J., Parslow, R. A., Patel, S., and Wheatley, M. (2000) *Biochemistry* **39,** 13524–13533
30. Kruszynski, M., Lammek, B., Manning, M., Seto, J., Haldar, J., and Sawyer, W. H. (1980) *J. Med. Chem.* **23,** 364–368
31. Serradeil-Le Gal, C., Wagnon, J., Garcia, C., Lacour, C., Guiraudou, P., Christophe, B., Villanova, G., Nisato, D., Maffrand, J. P., and Le Fur, G. P. (1993) *J. Clin. Invest.* **92,** 224–231
32. Ruan, K.-H., So, S.-P., Wu, J., Li, D., Huang, A., and Kung, J. (2001) *Biochemistry* **40,** 275–280
33. Zhang, L., DeHaven, R. N., and Goodman, M. (2002) *Biochemistry* **41,** 61–68
34. Pellegrini, M., Bremer, A. A., Ulfers, A. L., Boyd, N. D., and Mierke, D. F. (2001) *J. Biol. Chem.* **276,** 22862–22867
35. Lequin, O., Bolbach, G., Frank, F., Convert, O., Girault-Lagrange, S., Chassaing, G., Lavielle, S., and Sagan, S. (2002) *J. Biol. Chem.* **277,** 22386–22394
36. Davidson, F. F., Loewen, P. C., and Khorana, H. G. (1994) *Proc. Natl. Acad. Sci. U. S. A.* **91,** 4029–4033
37. Zeng, F. Y., Soldner, A., Schoneberg, T., and Wess, J. (1999) *J. Neurochem.* **72,** 2404–2414
38. Noda, K., Saad, Y., Graham, R. M., and Karnik, S. S. (1994) *J. Biol. Chem.* **269,** 6743–6752
39. Elling, C. E., Raffetseder, U., Nielsen, S. M., and Schwartz, T. W. (2000) *Biochemistry* **39,** 667–675
40. Cook, J. V., and Eidne, K. A. (1997) *Endocrinology* **138,** 2800–2806
41. Sharif, M., and Hanley, M. R. (1992) *Nature* **357,** 279–280
42. Hawtin, S. R., Davies, A. R. L., Matthews, G., and Wheatley, M. (2001) *Biochem. J.* **357,** 73–81
43. Ballesteros, J. A., and Weinstein, H. (1995) *Methods Neurosci.* **25,** 366–428
44. Patel, A. B., Crocker, E., Eilers, M., Hirshfeld, A., Sheves, M., and Smith, S. O. (2004) *Proc. Natl. Acad. Sci. U. S. A.* **101,** 10048–10053
45. Wurch, T., and Pauwels, P. J. (2000) *J. Neurochem.* **75,** 1180–1189
46. Zhao, M. M., Hwa, J., and Perez, D. M. (1996) *Mol. Pharmacol.* **50,** 1118–1126
47. Fourmy, D., Escrieut, C., Archer, E., Gales, C., Gigoux, V., Maigret, B., Moroder, L., Silvente-Poirot, S., Martinez, J., Fehrentz, J. A., and Pradayrol, L. (2002) *Pharmacol. Toxicol.* **91,** 313–320
48. Zhou, N., Luo, Z., Luo, J., Liu, D., Hall, J. W., Pomerantz, R. J., and Huang, Z. (2001) *J. Biol. Chem.* **276,** 42826–42833
49. Ballesteros, J. A., Shi, L., and Javitch, J. A. (2001) *Mol. Pharmacol.* **60,** 1–19
50. Cavalli, A., Fanelli, F., Taddei, C., DeBenedetti, P. G., and Cotecchia, S. (1996) *FEBS Lett.* **399,** 9–13
51. Birnbaumer, M. (1999) *Arch. Med. Res.* **30,** 465–474
52. Patel, A. B., Crocker, E., Reeves, P. J., Getmanova, E. V., Eilers, M., Khorana, H. G., and Smith, S. O. (2005) *J. Mol. Biol.* **347,** 803–812
53. Madabushi, S., Gross, A. K., Philippi, A., Meng, E. C., Wensel, T. G., and Lichtarge, O. (2004) *J. Biol. Chem.* **279,** 8126–8132
54. Klco, J. M., Wiegand, C. B., Narzinski, K., and Baranski, T. J. (2005) *Nat. Struct. Mol. Biol.* **12,** 320–326
55. Kleinau, G., Claus, M., Jaeschke, H., Mueller, S., Neumann, S., Paschke, R., and Krause, G. (2007) *J. Biol. Chem.* **282,** 518–525
56. Scarselli, M., Li, B., Kim, S.-K., and Wess, J. (2007) *J. Biol. Chem.* **282,** 7385–7396

Systematic Analysis of the Entire Second Extracellular Loop of the V_{1a} Vasopressin Receptor: KEY RESIDUES, CONSERVED THROUGHOUT A G-PROTEIN-COUPLED RECEPTOR FAMILY, IDENTIFIED

Matthew Conner, Stuart R. Hawtin, John Simms, Denise Wootten, Zoe Lawson, Alex C. Conner, Rosemary A. Parslow and Mark Wheatley

J. Biol. Chem. 2007, 282:17405-17412.
doi: 10.1074/jbc.M702151200 originally published online April 2, 2007
